Pressure-induced orthorhombic structure of PbS

2010 J. Phys.: Condens. Matter 22 095402

(http://iopscience.iop.org/0953-8984/22/9/095402)

J. Phys.: Condens. Matter **22** (2010) 095402 (6pp) doi:10.1088/0953-8984/22/9/095402

Pressure-induced orthorhombic structure of PbS

Andrzej Grzechnik[1] **and Karen Friese**

Departamento de Física de la Materia Condensada, Universidad del País Vasco, 48080 Bilbao, Spain

E-mail: andrzej.grzechnik@ehu.es

Received 16 November 2009, in final form 12 January 2010
Published 15 February 2010
Online at stacks.iop.org/JPhysCM/22/095402

Abstract

The pressure-induced crystal structure of lead sulfide (PbS) above 2.2 GPa has been studied with single-crystal x-ray diffraction in a diamond anvil cell at room temperature. It has been found to be twinned and of the TlI type ($Cmcm$, $Z = 4$), in which the Pb atoms are surrounded by seven S atoms in a capped trigonal prism coordination. The twin laws in relation to the parent B1 (NaCl) type structure ($Fm\bar{3}m$, $Z = 4$) at atmospheric pressure have been discussed.

(Some figures in this article are in colour only in the electronic version)

1. Introduction

At ambient conditions, lead chalcogenides PbS, PbSe and PbTe have the galena (B1, NaCl) structure ($Fm\bar{3}m$, $Z = 4$). They undergo first-order phase transitions to new polymorphs at about 2.2, 4.5 and 6.0 GPa, respectively [1–7]. Further transformations to the CsCl (B2) structure ($Pm\bar{3}m$, $Z = 1$) occur in them at 22.0, 16.0 and 13.0 GPa, respectively.

A powder x-ray diffraction study on PbTe [2] has shown that its polymorph existing between 6.0 and 13.0 GPa is a distorted variant of the NaCl structure ($Pnma$, $Z = 4$) in which the Pb atoms are sevenfold-coordinated to the Te atoms.

The crystal structures of the intermediate phases in PbS and PbSe are still controversial [1, 3–7]. Tolédano *et al* [8] have presented a phenomenological model for the transformations between the B1 and B2 types consisting of two consecutive displacive mechanisms coupled to tensile and shear strains. These mechanisms lead to intermediate structures of the TlI ($Cmcm$, $Z = 4$) or GeS ($Pnma$, $Z = 4$) types. The models by Tolédano *et al* [8] are, in principle, supported by the fact that the structure of TlI ($Cmcm$, $Z = 4$) can be discussed in relation to either the B1 [9] or the B2 [10] types. However, the experimental evidence for the occurrence of any of these two intermediates is contradictory. Maclean *et al* [11] have suggested that the intermediate structure in PbSe and PbS is a monoclinically distorted variant of the GeS type. On the other hand, Knorr *et al* [12] have postulated that β-PbS is of the TlI type. Both Maclean *et al* [11] and Knorr *et al* [12] have not been able to produce full-pattern Rietveld fits to their data to support their claims. In this context, it is worth noting that, in tin chalcogenides SnS and SnSe, the phase transition from the GeS type structure to the TlI one occurs at high temperatures and ambient pressure [13]. The transformation is of second order, mainly due to continuous displacements of all atoms almost exactly along the [100] direction.

Ponosov *et al* [14] have found out that the number of observed Raman modes for the intermediate polymorphs of PbS and PbSe is significantly smaller than expected from selection rules for the GeS type but it seems to be consistent with the TlI type. Interestingly, they have also observed optically that the surface of the PbS crystals compressed to above about 2.5 GPa develops a 'domain-like' pattern. The grain-size effect on the pressure-induced phase transitions in PbS galena has been studied by Qadri *et al* [15] and Jiang *et al* [16]. The onset of the phase transitions increases with decreasing particle size. According to electrical resistance measurements [17], the transformation in the bulk material occurs with little temperature variation.

Considering all the controversies regarding the pressure-induced intermediate polymorph of PbS in the transformation B1 $\leftrightarrow$ B2, we have been interested in solving its crystal structure above 2.2 GPa using single-crystal x-ray diffraction in a diamond anvil cell.

2. Experimental details

Several crystals of PbS galena were chosen from the material supplied by Alfa-Aesar (99.995%). Each of them was mounted on a glass pin and its single-crystal intensities were measured at room temperature using an STOE diffractometer IPDS-I

[1] Author to whom any correspondence should be addressed.

Table 1. Comparison of different structural models for PbS at 6.36 GPa. (Note: $R(\text{int}) = \sum_i \sum_j \frac{(I_j - \bar{I}_i)}{\bar{I}_i}$, where i runs over all independent reflections and j over all equivalent reflections corresponding to the ith independent reflection. Note that j need not to be the same for all independent reflections, $R = \frac{\sum_{hkl} ||F_o| - |F_c||}{\sum_{hkl} |F_o|}$, R(obs): for observed reflections $I > 3\sigma$; R(all): for all reflections, weighted R factor $wR = \sqrt{\frac{\sum_{hkl} w[I_o - I_c]^2}{\sum_{hkl} wI_o^2}}$, wR(obs): for observed reflections $I > 3\sigma$; wR(all): for all reflections.)

Space group	R(int) obs	R(int) all	No. reflections obs/all	No. rejected reflections	Redundancy	R(obs)	wR(obs)	R(all)	wR(all)	No. par.	Remark
$P21/n$	0.0966	0.1445	47/119	—	6.319	0.1390	0.1341	0.3791	0.1368	8	Pb iso
$P21/n$	0.0966	0.1445	47/119	—	6.319	0.1028	0.1040	0.4174	0.1112	12	Pb aniso
$P21/n$	0.0931	0.1404	52/129	—	5.829	0.1028	0.1040	0.4174	0.1112	12	Six twin laws
$Cmcm$	0.1750	0.1860	29/45	17	9.822	0.088	0.0766	0.1415	0.0775	5	No twin
$Cmcm$	0.1367	0.1669	42/87	—	7.000	0.1136	0.0981	0.3088	0.1022	10	Six twin laws
$Cmcm$	0.1393	0.1557	40/65	4	7.400	0.1164	0.1154	0.1905	0.1162	6	Twofold rotation around $[21\bar{2}]$

(Mo Kα: 0.710 73 Å). The intensity data of all the crystals were then evaluated and compared with those by Noda *et al* [18]. The crystal of the best quality was selected for further high-pressure studies.

Single-crystal intensities at high pressures were measured from the selected crystal (approximately $60 \times 50 \times 30\ \mu m^2$) in the Ahsbahs-type diamond anvil cell [19] at room temperature using an STOE diffractometer IPDS-2T (Mo Kα: 0.710 73 Å). A 250 μm hole was drilled into a stainless steel gasket preindented to a thickness of about 80 μm. The intensities were indexed, integrated and corrected for absorption using the STOE software [20]. Shaded areas of the images by the diamond anvil cell were masked prior to integration. The intensities were integrated simultaneously with three orientation matrices, corresponding to the crystal of PbS and to the two diamonds of the cell. Due to their hemispherical shape, no absorption correction was necessary for the diamond anvils [19]. The ruby luminescence method [21] was used for pressure calibration and a 4:1 mixture of methanol and ethanol was used as a pressure medium. The ambient-pressure room-temperature data after compression were measured from the same crystal mounted on a glass pin using the IPDS-2T diffractometer (Mo Kα: 0.710 73 Å).

All the data were analyzed and refined using the program JANA2006 [22][2].

3. Results and discussion

Considering the fact that the high-pressure behavior and the equation of state of the cubic form of PbS has been studied in detail previously [12], the crystal of PbS was compressed initially to 2.86 GPa, i.e. to the pressure slightly above the phase transition. In total, five datasets were collected up to 7.73 GPa. The diffraction diagrams at all pressures could be indexed with a primitive orthorhombic cell with approximate lattice parameters of $a \approx 4.0$ Å, $b \approx 11.2$ Å and $c \approx 4.2$ Å. A slight splitting of reflections indicated additional pseudomerohedral twinning: however, it was not possible to separate the reflections of different domains in the integration process. Assuming an untwinned structure, the systematic extinctions [22] and the internal agreement R(int) factor indicated a space group $P12_1/n1$ with a monoclinic angle $\beta \approx 90°$. The structure could indeed be solved in this space group using direct methods [22] without any problems.

For further structural analysis of the new polymorph of PbS, we used the dataset collected at 6.36 GPa, with altogether 475 measured reflections, of which 303 are observed on the basis of a 3σ criterion. In the initial refinement, the following parameters were included: positional parameters of the Pb and S atoms, (an)isotropic thermal parameters of the Pb atom, an isotropic thermal parameter of the S atom and a scale factor (table 1). The main problem of these models is the high agreement R factor for the unobserved reflections that are calculated with relatively high intensities.

Considering group–subgroup relations, one might assume that the reduction of the point group symmetry from $m\bar{3}m$ to the point group symmetry $2/m$ converts the lost symmetry elements into potential twin operations with 12 different twin laws. However, given the limited number of reflections available due to an opening angle of the diamond anvil cell of 90°, a simultaneous refinement of all of the corresponding volume fractions was not feasible. The limited information about the reciprocal space implies that it was not possible to deduce the twin laws reliably, based on the analysis of the observed splitting of reflections. We therefore chose a trial-and-error approach and tested different twin laws separately and in different combinations. It became evident that only a set of six matrices could be used in the refinement, the other set of six matrices being related by a 180° rotation around [001]. This was reflected in the fact that simultaneous refinement of volume fractions of twin matrices related by this symmetry operation led to large correlations and unreasonable values.

[2] Further details of the crystallographic investigations can be obtained from the Fachinformationszentrum Karlsruhe, D-76344 Eggenstein-Leopoldshafen, Germany, on quoting the depository numbers CSD 421423.

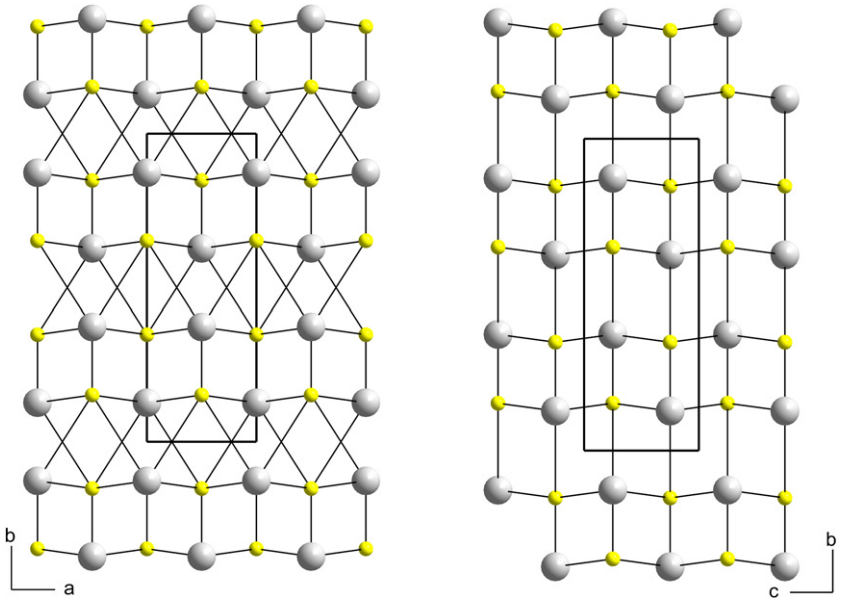

Figure 1. Crystal structure of PbS at 6.36 GPa ($Cmcm$, $Z = 4$). The gray and yellow symbols represent the Pb and S atoms, respectively.

All obtained models exhibited a strong pseudosymmetry with respect to space group $C2/c$, one of the minimal supergroups of $P2_1/n$, according to the pseudosymmetry search using the program PSEUDO on the Bilbao Crystallographic Server[3,4]. In addition, in space group $C2/c$, all atoms would occupy non-characteristic orbits so that the monoclinic structure is, in fact, equivalent to the orthorhombic structure in space group $Cmcm$ (provided that $\beta = 90°$). The change of the space group symmetry from $P2_1/n$ to $Cmcm$ implies that the atoms move from the Wyckoff positions 4e (x, y, z) in space group $P2_1/n$ to the Wyckoff positions 4c $(0, y, 1/4)$ in the orthorhombic one.

The behavior of the twin volume fractions mentioned earlier and the pseudosymmetry of the structure suggested a point group symmetry mmm for the high-pressure polymorph of PbS. Earlier results from powder diffraction indicated a space group $Cmcm$ of the TlI structural type as a reasonable candidate [12], while the metrics we obtained from our single-crystal data showed no deviation of the monoclinic angle from 90° at all pressures. However, there are 17 observed reflections which violate the extinction rules for the C-centered lattice in our data. In addition, the R(int) value is comparatively high, assuming point group symmetry mmm and huge discrepancies are observed for some of the intensities of symmetry equivalent reflections. These observations thus suggest that additional twinning has to be taken into account if space group $Cmcm$ is chosen.

Although the involved space groups $Fm\bar{3}m$ and $Cmcm$ are not in a group–subgroup relation, it is easy to deduce six different twin laws corresponding to the lost rotational symmetry operations. The inclusion of these twin laws explains all the 17 systematic absence violations. In the refinements it is possible to include the volume fractions corresponding to the six individuals, although at the cost of a bad parameter-to-data ratio (table 1). Apart from that, the refinement leads to a high overall agreement factor for the unobserved reflections (>30%), so that the model is not satisfactory.

Table 2. Atomic coordinates and isotropic displacement parameters for PbS at 6.36 GPa: $a = 4.008(4)$ Å, $b = 11.246(23)$ Å and $c = 4.154(4)$ Å. The structural model is in space group $Cmcm$ ($Z = 4$) with twofold rotation around the $[21\bar{2}]$ direction as a twin operation.

Atom	x	y	z	U_{iso}
Pb	0.0	0.127(3)	0.25	0.042(4)
S	0.0	0.348(13)	0.25	0.02(1)

A closer inspection and comparison of the intensities of symmetry equivalent reflections in $Cmcm$ suggested a twin law corresponding to a 180° rotation around the orthorhombic $[21\bar{2}]$ direction, which in turn corresponds to the cubic [110] direction. The introduction of this twin explains the majority of the systematic absence violations[5]. Its advantage is that only one additional parameter has to be taken into account. The agreement factor for the unobserved reflections drops drastically when compared to the other model in $Cmcm$ with six twin laws (table 1).

Since the shifts of both Pb and S atoms from their position in $P2_1/n$ towards the ones in $Cmcm$ are small due to the high pseudosymmetry of the $P2_1/n$ structure, we do not observe a substantial influence on the overall agreement factors of the refinements (table 1). It is also important to point out that

[3] www.cryst.ehu.es

[4] The GeS type structure ($Pnma$, $Z = 4$) has a very high pseudosymmetry with respect to space group $Cmcm$ as obtained using the program PSEUDO. See [13] for further information regarding the transformation $Pnma \rightarrow Cmcm$.

[5] The remaining four reflections violating the C-centered lattice can be readily explained by introducing a second twin law. However, we abstained from doing so as this would lead to a worse parameter-to-data ratio and preferred to exclude these four reflections from the refinement.

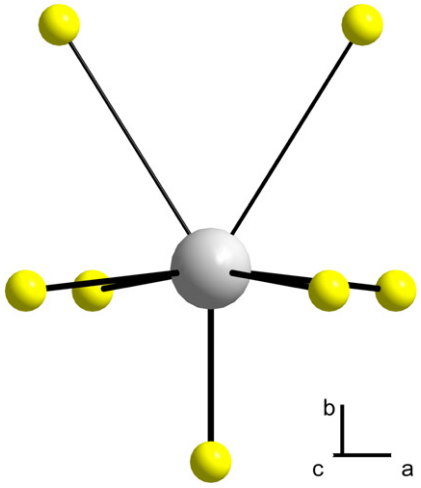

Figure 2. The coordination sphere of the Pb atom in PbS at 6.36 GPa. The Pb–S distances below 3 Å are marked with thick lines.

Table 3. Interatomic distances for PbS at 6.36 GPa. The structural model is in space group $Cmcm$ ($Z = 4$) with twofold rotation around the $[21\bar{2}]$ direction as a twin operation.

Distance (Å)		
Pb–S		2.49(1)
	4x	2.90(2)
	2x	3.72(1)
Pb–Pb	2x	3.53(4)
	4x	4.00(3)

all three models in $Cmcm$ lead (within the estimated standard deviations) to identical atomic coordinates and displacement parameters for both Pb and S atoms (table 2).

The crystal structure of PbS at 6.36 GPa, described in space group $Cmcm$ ($Z = 4$) with an additional twofold rotation around the $[21\bar{2}]$ direction as a twin operation, is of the TlI type (figure 1 and tables 2 and 3). Each of the Pb atoms is surrounded by seven S atoms in the form of a capped trigonal prism (the coordination $1 + 4 + 2$) (figure 2 and table 3). The height of the prism is determined by the a lattice parameter [23, 24]. The S atom that caps the prism gives the shortest Pb–S distance along the b axis. When only the Pb–S distances below 3 Å are taken into account, the structure could be considered as a stack of layers in the b direction.

The same capped trigonal prism coordination of the cation to the anions is also present in PbTe ($Pnma$, $Z = 4$) [2]. However, the pressure-induced crystal structure of lead telluride cannot be interpreted as being layered. Disregarding the shortest Pb–S distances, the face-sharing trigonal prisms form layers in PbS ($Cmcm$, $Z = 4$), while the columns of face-sharing trigonal prisms are connected by edges to form a three-dimensional structure in PbTe ($Pnma$, $Z = 4$) [2].

It is also worth mentioning that the PbS subsystems in several misfit layer compounds at atmospheric pressure have symmetries $Cm2a$ [25], $Cmc2_1$ [26] or $C121$ [27], all of them being the subgroups of space group $Cmcm$. The distortions of the misfit PbS layer in these materials are quite similar to those

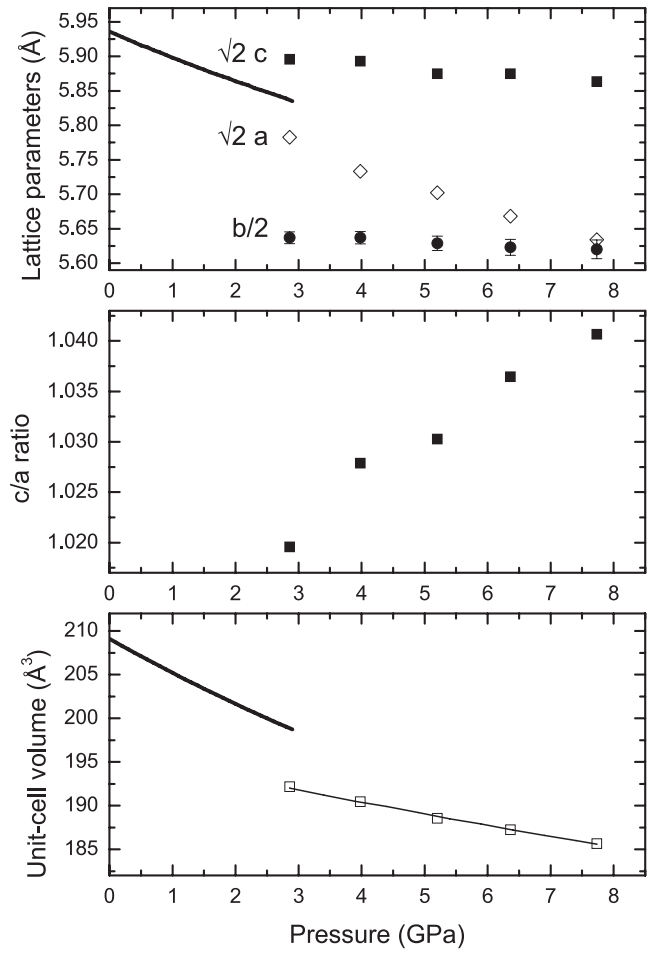

Figure 3. Pressure dependence of lattice parameters, axial c/a ratio and unit-cell volumes for the $Fm\bar{3}m$ and $Cmcm$ phases of PbS. The lattice parameters for the orthorhombic polymorph are plotted as $\sqrt{2}a$, $b/2$ and $\sqrt{2}c$. The error bars are shown when larger than the size of the data points. The thick lines correspond to the calculated Birch–Murnaghan equation of state and lattice parameter using the bulk modulus $B_0 = 51$ GPa and its first pressure derivative $B' = 4.3$ from [12] and the zero-pressure unit-cell volume $V_0 = 209.2(1)$ Å^3 from this study. The thin line represents the second-order Birch–Murnaghan equation of state with $B_{tr} = 134(2)$ GPa and $V_{tr} = 192.1(4)$ Å^3 for $B'_{tr} = 4.00$ at $P_{tr} = 2.86$ GPa.

in the high-pressure structure of bulk PbS. On the other hand, a distorted PbS lattice occurs in modular structures of sulfosalt minerals [28].

The lattice parameter and unit-cell volume of PbS at ambient pressure are $a = 5.936(1)$ Å and $V = 209.2(1)$ Å^3. The parameters of the third-order Birch–Murnaghan equation of state (EoS) of galena are $B_0 = 51(1)$ GPa and $B' = 4.3(9)$ [12]. Figure 3 shows the pressure dependence of lattice parameters and unit-cell volumes for both $Fm\bar{3}m$ and $Cmcm$ phases of PbS. Since the zero-pressure volume V_0 for orthorhombic PbS cannot be well determined from the EoS fit, a modified second-order Birch–Murnaghan EoS in terms of $(P - P_{tr})$ [29], where $P_{tr} = 2.86$ GPa is the transition pressure, was used. As a result, the bulk modulus $B_{tr} = 134(2)$ GPa and the unit-cell volume $V_{tr} = 192.1(4)$ Å^3 for $B'_{tr} = 4.00$ are evaluated at $P_{tr} = 2.86$ GPa. The relative unit-cell volume

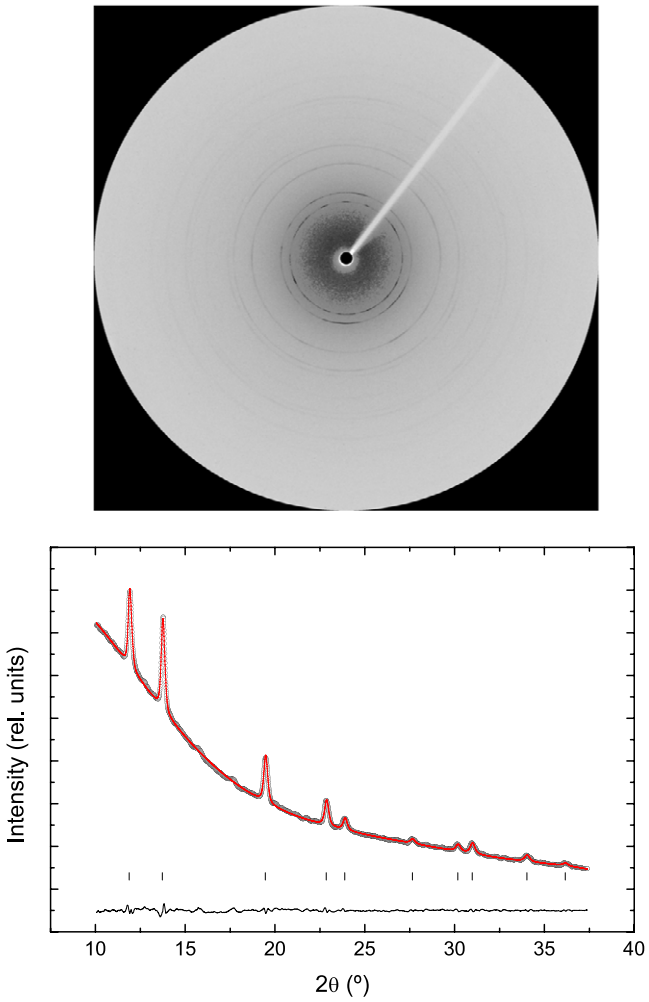

Figure 4. A Gandolfi-like diffraction diagram of the PbS single crystal decompressed from 7.73 GPa (top) and the corresponding integrated powder diagram refined with the Le Bail method assuming the $Fm\bar{3}m$ lattice (bottom). Vertical markers indicate Bragg reflections.

change due to the $Fm\bar{3}m \rightarrow Cmcm$ phase transition at 2.86 GPa, assuming the EoS from [12] and from this study, is -3.3%.

The orthorhombic crystal structure of PbS has an anisotropic compressibility, with the a lattice parameter being the most compressible (figure 3). On the other hand, some other compounds of the TlI type are softer perpendicular to the b direction [23, 24], i.e. they compress more within the quasi-layer due to Pb and S atomic displacements along the b axis. According to [23, 24], the a lattice parameter determines the cation–anion interactions, while the c lattice parameter is strongly correlated with the cation–cation and anion–anion interactions. Like in TlI itself [24], the axial ratio c/a in orthorhombic PbS increases upon compression, indicating that the trigonal prism coordination sphere around the Pb atom is more sensitive to the unit-cell volume changes than the atomic interactions along the c axis.

To confirm whether the first-order phase transition $Fm\bar{3}m \rightarrow Cmcm$ is reversible, as previously indicated in [1, 12], diffraction data at atmospheric pressure were measured from the crystal decompressed from 7.73 GPa and mounted on a glass pin. The observed reflections were largely smeared but nevertheless indexable with the $Fm\bar{3}m$ lattice. However, due to the deterioration of the crystal, it was not possible to obtain reliably integrated single-crystal diffraction intensities from the crystal on decompression. Figure 4 shows a Gandolfi-type diagram [30] collected using the ω oscillations in the range 0°–180°, in which the Debye–Scherrer rings of PbS galena are clearly visible. The integrated powder pattern using the STOE software [20] could be well refined with the Le Bail method [31] assuming the cubic lattice.

4. Conclusions

PbS galena with the B1 (NaCl) structure ($Fm\bar{3}m$, $Z = 4$) undergoes a phase transition to a crystal structure of the TlI type ($Cmcm$, $Z = 4$) above 2.2 GPa, with the Pb atoms in the new polymorph sevenfold-coordinated to the S atoms. The structure is affected by additional twinning.

Our data give a definitive answer about the structural arrangement of the atoms in the high-pressure polymorph of PbS. As the twin laws might provide further information about the underlying structural mechanism of the B1 $\leftrightarrow$ B2 phase transition, further theoretical and experimental investigations are warranted.

Acknowledgments

The authors thank E Makovicky for discussions. They also acknowledge the Universidad del País Vasco, the Gobierno Vasco and the Ministerio de Ciencia e Innovación for supporting their high-pressure laboratory.

References

[1] Chattopadhyay T, von Schnering H G, Grosshans W A and Holzapfel W B 1986 *Physica* B **139/140** 386
[2] Rousse G, Klotz S, Saitta A M, Rodriguez-Carvajal J, McMahon M I, Couzinet B and Mezouar M 2005 *Phys. Rev.* B **71** 2241161
[3] Ahuja R 2003 *Phys. Status Solidi* b **235** 341
[4] Grzechnik A 2007 *Pressure-Induced Phase Transitions* ed A Grzechnik (Kerala: Transworld Research Network)
[5] Ovsyannikov S V, Shchennikov V V, Manakov A Y, Likhacheva A Y, Berger I F, Ancharov A I and Sheromov M A 2007 *Phys. Status Solidi* b **244** 279
[6] Streltsov S V, Manakov A Yu, Vokhmyanin A P, Ovsyannikov S V and Shchennikov V V 2009 *J. Phys.: Condens. Matter* **21** 385501
[7] Ovsyannikov S V, Shchennikov V V, Manakov A Y, Likhacheva A Y, Ponosov Y S, Mogilenskikh V, Vokhmyanin A P, Ancharov A I and Skipetrov E P 2009 *Phys. Status Solidi* b **246** 615
[8] Tolédano P, Knorr K, Ehm L and Depmeier W 2003 *Phys. Rev.* B **67** 144106
[9] van der Vorst C P J M and Maaskant W J A 1980 *J. Solid State Chem.* **34** 301
[10] Becker D and Beck H B 2004 *Z. Anorg. Allg. Chem.* **630** 41
[11] Maclean J, Hatton P D, Piltz R O, Crain J and Cernik R J 1995 *Nucl. Instrum. Methods Phys. Res.* B **97** 354
[12] Knorr K, Ehm L, Hytha M, Winkler B and Depmeier W 2003 *Eur. Phys. J.* B **31** 297

[13] Chattopadhyay T, Pannetier J and von Schnering H G 1986 *J. Phys. Chem. Solids* **47** 879
[14] Ponosov Yu S, Ovsyannikov S V, Streltsov S V, Shchennikov V V and Syassen K 2009 *High Pressure Res.* **29** 224
[15] Qadri S B, Yang J, Ratna B R, Skelton E F and Hu J Z 1996 *Appl. Phys. Lett.* **69** 2205
[16] Jiang J Z, Gerward L, Secco R, Frost D, Olsen J S and Truckenbrodt J 2000 *J. Appl. Phys.* **87** 2658
[17] Wheeler K T, Walker D and Johnson M C 2007 *Am. J. Sci.* **307** 590
[18] Noda Y, Masumoto K, Ohba S, Saito Y and Toriumi K 1987 *Acta Crystallogr.* C **43** 1443
[19] Ahsbahs H 1995 *Z. Kristallogr.* **Suppl. 9** 42
Ahsbahs H 2004 *Z. Kristallogr.* **219** 305
[20] X-AREA *Stoe IPDS Software* Stoe and Cie GmbH, Darmstadt, Germany
[21] Piermarini G J, Block S, Barnett J D and Forman R A 1975 *J. Appl. Phys.* **46** 2774
Mao H K, Xu J and Bell P M 1986 *J. Geophys. Res.* **91** 4673
[22] Petricek V, Dusek M and Palatinus L 2006 *The Crystallographic Computing System* (Praha: Institute of Physics)
[23] Becker D and Beck H P 2004 *Z. Anorg. Allg. Chem.* **630** 41
[24] Becker D and Beck H P 2004 *Z. Kristallogr.* **219** 348
[25] Wiegers G A, Meetsma A, Haange R J, Van Smaalen S, de Boer J L, Meerschaut A, Rabu P and Rouxel J 1990 *Acta Crystallogr.* B **46** 324
[26] Meerschaut A, Guemas L, Auriel C and Rouxel J 1990 *Eur. J. Solid State Inorg. Chem.* **27** 557
[27] Onoda M, Kato K, Gotoh Y and Oosawa Y 1990 *Acta Crystallogr.* B **46** 487
[28] Elcoro L, Perez-Mato J M, Friese K, Petricek V, Balic-Zunic T and Olsen L A 2008 *Acta Crystallogr.* B **64** 684
[29] Menoni C S, Hu J Z and Spain I L 1986 *Phys. Rev.* B **34** 362
[30] Giacovazzo C (ed) 2002 *Fundamentals of Crystallography* 2nd edn (Oxford: Oxford University Press)
[31] LeBail A, Duroy H and Fourquet J L 1988 *Mater. Res. Bull.* **23** 447